nature medicine

Peroxiredoxin family proteins are key initiators of post-ischemic inflammation in the brain

Takashi Shichita[1–3], Eiichi Hasegawa[1], Akihiro Kimura[1], Rimpei Morita[1], Ryota Sakaguchi[1], Ichiro Takada[1], Takashi Sekiya[1], Hiroaki Ooboshi[4], Takanari Kitazono[3], Toru Yanagawa[5], Tetsuro Ishii[5], Hideo Takahashi[6], Shuji Mori[6], Masahiro Nishibori[6], Kazumichi Kuroda[7], Shizuo Akira[8], Kensuke Miyake[9] & Akihiko Yoshimura[1,10]

Post-ischemic inflammation is an essential step in the progression of brain ischemia-reperfusion injury. However, the mechanism that activates infiltrating macrophages in the ischemic brain remains to be clarified. Here we demonstrate that peroxiredoxin (Prx) family proteins released extracellularly from necrotic brain cells induce expression of inflammatory cytokines including interleukin-23 in macrophages through activation of Toll-like receptor 2 (TLR2) and TLR4, thereby promoting neural cell death, even though intracellular Prxs have been shown to be neuroprotective. The extracellular release of Prxs in the ischemic core occurred 12 h after stroke onset, and neutralization of extracellular Prxs with antibodies suppressed inflammatory cytokine expression and infarct volume growth. In contrast, high mobility group box 1 (HMGB1), a well-known damage-associated molecular pattern molecule, was released before Prx and had a limited role in post-ischemic macrophage activation. We thus propose that extracellular Prxs are previously unknown danger signals in the ischemic brain and that its blocking agents are potent neuroprotective tools.

Stroke is one of the major causes of death and disability worldwide. The only globally approved treatment for ischemic stroke is tissue plasminogen activator, a time-dependent therapy that must be given within 4.5 h of stroke onset. Consequently, there is an unmet need for therapy that could be commenced beyond this time window and that would be aimed at brain tissue protection rather than clot dissolution[1–3].

Recent evidence suggests that various elements of the immune system are intimately involved in all stages of the ischemic cascade, from the acute intravascular events to the parenchymal processes leading to brain damage and tissue repair, which determine the fate of patients after stroke[4–6]. In mouse models, immune cells such as T cells and macrophages and their cytokines have been shown to have a pivotal role in the immunomodulation of post-ischemic inflammation[7–10]. We have reported that interleukin-23 (IL-23) produced from infiltrating macrophages induces IL-17–producing T cells. IL-17 is mainly produced from γδT cells and promotes delayed (day 3–4) ischemic brain damage[11,12].

Despite intensive study of post-ischemic inflammation, the molecular mechanisms that activate infiltrating macrophages remain unclear. TLRs are pivotal in triggering the inflammation of sterile organs[13,14]. HMGB1, heat shock proteins (HSPs), β-amyloid (Aβ) and others are well known as endogenous TLR ligands; that is, they are damage-associated molecular pattern molecules (DAMPs)[15–19]. Although HMGB1 is implicated in ischemic brain injury, it remains to be clarified whether HMGB1 is the major DAMP involved in the activation of infiltrating immune cells or whether other local DAMPs have roles in this process[20–23].

In this study, we identified Prx family proteins in brain lysate as strong inducers of inflammatory cytokines. The extracellular release of Prx proteins occurred 12 h after stroke onset, which coincided with the timing of macrophage infiltration and stimulated infiltrating macrophages via TLR2 and TLR4. Neutralization of Prx proteins rather than HMGB1 by specific antibodies suppressed inflammatory cytokine expression in the ischemic brain. Thus, extracellular Prx could be a previously unknown DAMP that triggers post-ischemic inflammation and an ideal therapeutic target for ischemic brain injury.

RESULTS

Peroxiredoxins are potent IL-23 inducers in brain lysate

To determine whether there are DAMPs that induce IL-23 in the brain, we cultured bone marrow–derived dendritic cells (BMDCs) with a brain homogenate supernatant (brain lysate) from mice. mRNA encoding IL-23 p19 and other cytokine mRNAs were rapidly induced in BMDCs by incubation with the brain lysate (**Fig. 1a** and

[1]Department of Microbiology and Immunology, School of Medicine, Keio University, Tokyo, Japan. [2]Precursory Research for Embryonic Science and Technology (PRESTO), Japan Science and Technology Agency, Tokyo, Japan. [3]Department of Medicine and Clinical Science, Graduate School of Medical Sciences, Kyushu University, Fukuoka, Japan. [4]Department of Internal Medicine, Fukuoka Dental College Medical and Dental Hospital, Fukuoka, Japan. [5]Faculty of Medicine, University of Tsukuba, Tsukuba, Japan. [6]Department of Pharmacology, Okayama University Graduate School of Medicine, Okayama, Japan. [7]Division of Microbiology, Nihon University School of Medicine, Tokyo, Japan. [8]Laboratory of Host Defense, WPI Immunology Frontier Research Center, Osaka University, Osaka, Japan. [9]Division of Infectious Genetics, Institute of Medical Science, University of Tokyo, Tokyo, Japan. [10]Core Research for Evolutional Science and Technology (CREST), Japan Science and Technology Agency, Tokyo, Japan. Correspondence should be addressed to A.Y. (yoshimura@a6.keio.jp).

Received 23 January; accepted 21 March; published online 20 May 2012; doi:10.1038/nm.2749

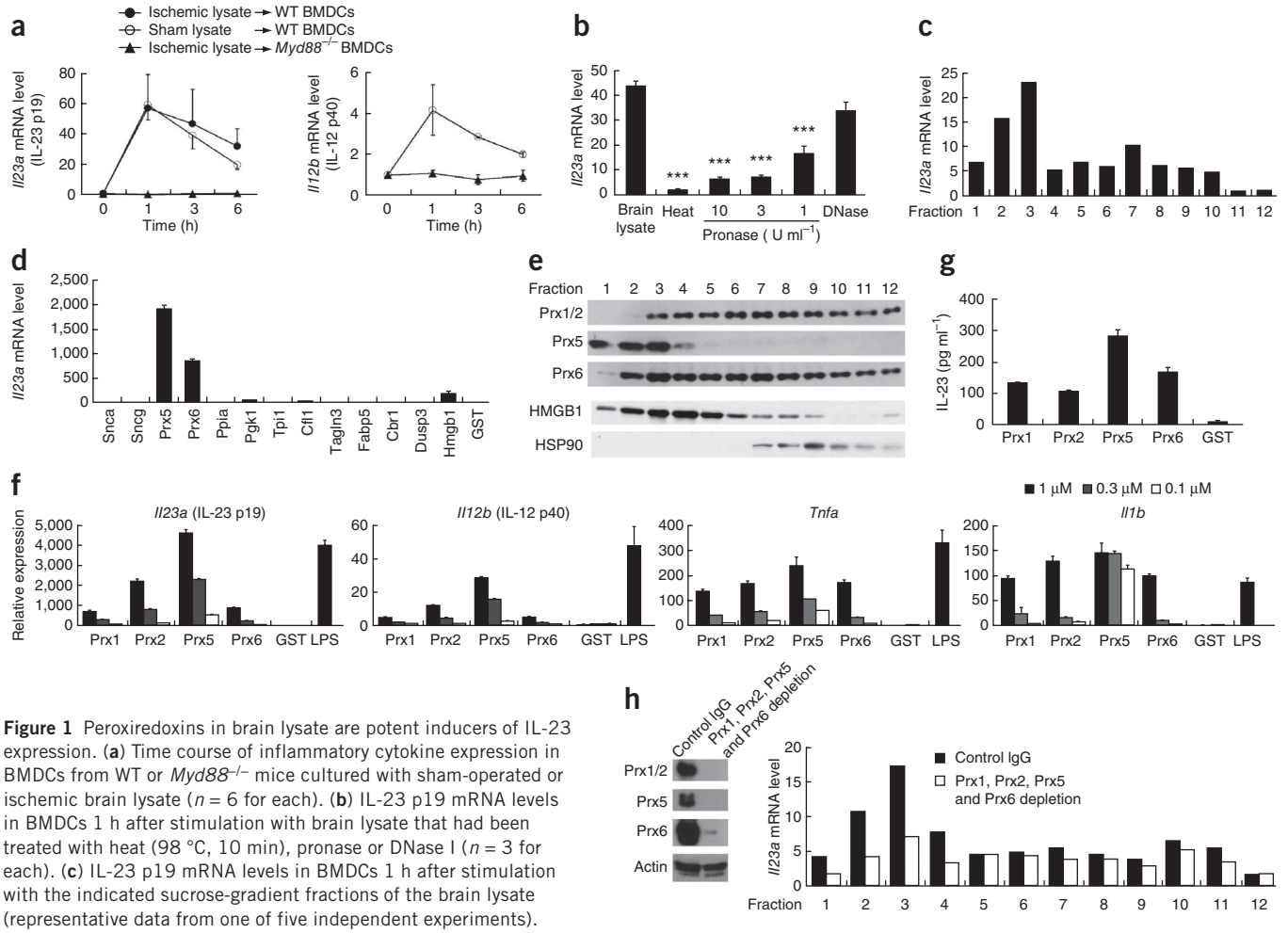

Figure 1 Peroxiredoxins in brain lysate are potent inducers of IL-23 expression. (**a**) Time course of inflammatory cytokine expression in BMDCs from WT or *Myd88*$^{-/-}$ mice cultured with sham-operated or ischemic brain lysate ($n = 6$ for each). (**b**) IL-23 p19 mRNA levels in BMDCs 1 h after stimulation with brain lysate that had been treated with heat (98 °C, 10 min), pronase or DNase I ($n = 3$ for each). (**c**) IL-23 p19 mRNA levels in BMDCs 1 h after stimulation with the indicated sucrose-gradient fractions of the brain lysate (representative data from one of five independent experiments). (**d**) IL-23 p19 mRNA levels in BMDCs 1 h after stimulation with the indicated recombinant GST-fusion proteins ($n = 3$ for each) that are detected in sucrose-gradient fractions 2 and 3 by LC-MS. (**e**) Western blot analysis of the indicated proteins in the sucrose-gradient fraction of the brain lysate. (**f**,**g**) mRNA levels of inflammatory cytokines (**f**) and IL-23 protein levels (**g**) induced in BMDC by the addition of recombinant Prxs or GST protein or lipopolysaccharide (LPS, 100 ng ml^{-1}) ($n = 3$ for each). (**h**) IL-23 p19–inducing activity of each sucrose gradient fraction after immunoprecipitation using control IgG or the Prx-specific antibody mixture. The depletion of Prxs was confirmed by western blot analysis (left; representative data from two independent experiments). Each mRNA expression level indicates relative expression compared to that in untreated BMDCs. ***$P < 0.001$ versus brain lysate (one-way analysis of variance (ANOVA) with Dunnett's correction; the error bars represent s.e.m.).

Supplementary Fig. 1). We detected IL-23 p19–inducing activity in both ischemic and sham-operated brain lysates, suggesting that IL-23 inducers were released by the homogenization process of the brain. Furthermore, IL-23 p19–inducing activity was completely dependent on myeloid differentiation factor 88 (MyD88), an adaptor protein for TLR signaling pathway, both *in vitro* and *in vivo*, as IL-23 mRNA induction disappeared in MyD88-deficient BMDCs (**Fig. 1a**) and in the infiltrating immune cells collected by Percoll-gradient centrifugation from the ischemic brains of MyD88-deficient mice (**Supplementary Fig. 2**). These results suggest that IL-23 p19 expression was induced in a TLR-dependent manner by DAMPs released from damaged brain tissue.

Next, we tried to identify the DAMPs in the brain lysate. We determined that the IL-23–inducing DAMPs must be proteins, given that the IL-23 p19–inducing activity was almost completely diminished by heat or pronase treatment (**Fig. 1b**). Fractionation of the brain lysate revealed that IL-23 p19–inducing activity was present in the cytosolic fraction, that the protein in question did not bind a DEAE-Sepharose column and that its molecular weight was over 10 kDa (**Supplementary Fig. 3a**,**b**). After sucrose density gradient centrifugation, fractions 2 and 3, which contained mostly 15–25 kDa proteins (**Supplementary Fig. 4**), showed high IL-23 p19–inducing activity (**Fig. 1c**). Further analysis by liquid chromatography–mass spectrometry (LC-MS) identified more than 15 proteins that appeared more often in fractions 2 and 3 than in fractions 1 and 4 (**Supplementary Table 1**). We generated recombinant GST-fusion versions of these proteins in bacteria. After extensive washing and filtration through a polymyxin B–Sepharose column, we detected almost no IL-23 p19–inducing activity in preparations containing GST alone or in several GST-fusion protein preparations (**Fig. 1d**). However, we found that Prx5 and Prx6 had potent IL-23 p19–inducing activity compared to HMGB1 (**Fig. 1d**).

Characterization of Prx family proteins as IL-23 inducers

On the basis of these observations, and also because Prx1 was reported to activate macrophages via TLR4 (ref. 24), we decided to investigate whether Prx family proteins contribute to IL-23 production in brain lysates. First, we generated specific antibodies to

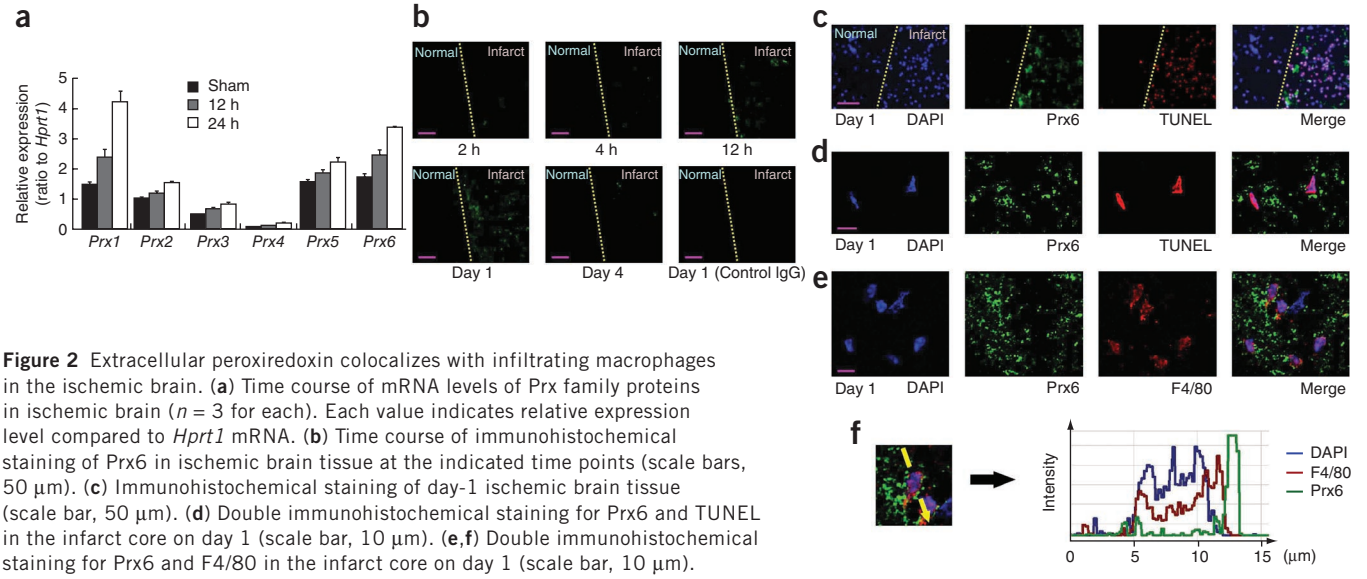

Figure 2 Extracellular peroxiredoxin colocalizes with infiltrating macrophages in the ischemic brain. (**a**) Time course of mRNA levels of Prx family proteins in ischemic brain ($n = 3$ for each). Each value indicates relative expression level compared to *Hprt1* mRNA. (**b**) Time course of immunohistochemical staining of Prx6 in ischemic brain tissue at the indicated time points (scale bars, 50 μm). (**c**) Immunohistochemical staining of day-1 ischemic brain tissue (scale bar, 50 μm). (**d**) Double immunohistochemical staining for Prx6 and TUNEL in the infarct core on day 1 (scale bar, 10 μm). (**e**,**f**) Double immunohistochemical staining for Prx6 and F4/80 in the infarct core on day 1 (scale bar, 10 μm). The graph in **f** shows a quantification of fluorescence intensity along the yellow arrow in left panel. The images were captured by using conventional fluorescence microscopy (**b**,**c**) or confocal laser microscopy (**d**–**f**). The error bars represent s.e.m.

Prx1 and Prx2 (Prx1/2), Prx5 and Prx6 by immunizing rabbits with recombinant Prx proteins. Our Prx1-specific antibody cross-reacted with Prx2 because of the high homology between Prx1 and Prx2, as previously reported[25] (**Supplementary Fig. 5**). Western blotting analysis revealed that Prx5 and Prx6 were most abundant in sucrose-gradient fractions 2 and 3 (**Fig. 1e**). Prx1 and Prx2 were broadly distributed but also detected in fractions 2 and 3. The highest incidence of HMGB1 and HSP90 in the sucrose density gradient was in fractions 4 and 9, respectively. These data suggest that Prx5, Prx6 and, to a lesser degree, Prx1/2 could contribute to the IL-23 induction achieved by fractions 2 and 3.

We then characterized the inflammatory cytokine–inducing activity of GST-free cleaved recombinant Prxs. Among these Prxs, recombinant Prx5 had the greatest activity in inducing the mRNA expression and production of IL-23 and other inflammatory cytokines, although other Prx family proteins could also induce both mRNA and protein expression of inflammatory cytokines in BMDCs (**Fig. 1f**,**g**). To confirm that Prxs are major inducers of IL-23 expression in the brain

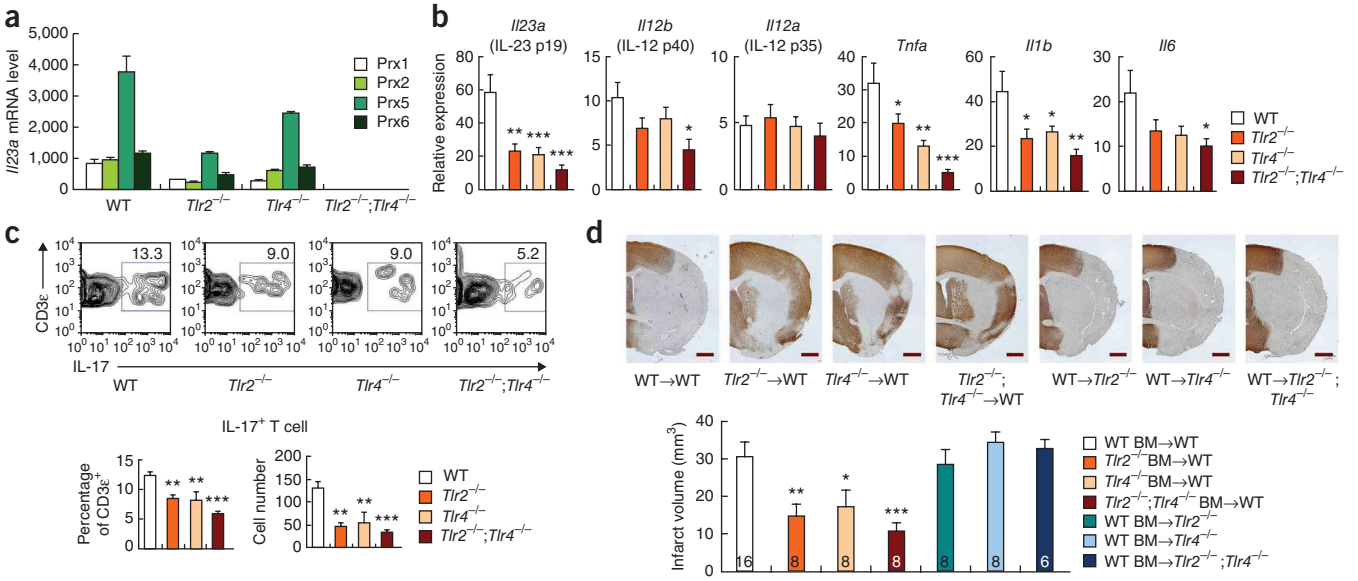

Figure 3 Peroxiredoxins induce IL-23 expression via TLR2 and TLR4. (**a**) IL-23 p19 mRNA levels in WT, TLR2-deficient, TLR4-deficient or TLR2 and TLR4 double-deficient BMDC 1 h after stimulation with 1 μM recombinant Prx proteins ($n = 4$ for each), shown relative to those in untreated BMDCs. (**b**) The mRNA levels of inflammatory cytokines in the infiltrating immune cells on day 1 after stroke onset ($n = 7$ for each). Each value indicates relative expression compared to that in sham-operated mice. (**c**) The ratio and the absolute number of IL-17$^+$ T cells on day 3 after stroke onset ($n = 8$ for WT and $n = 6$ for other samples). (**d**) Infarct volume (bottom) measured by MAP2 immunostaining of brain sections on day 4 after stroke onset in chimeric mice (top; scale bars, 1 mm). *Tlr2*$^{-/-}$ BM → WT means transfer of *Tlr2*$^{-/-}$ bone marrow cells into WT mice. The number of mice is shown on each bar. $^*P < 0.05$, $^{**}P < 0.01$, $^{***}P < 0.001$ versus WT mice (**b**,**c**) and WT bone marrow–transferred WT mice (**d**) (one-way ANOVA with Dunnett's correction; the error bars represent s.e.m.).

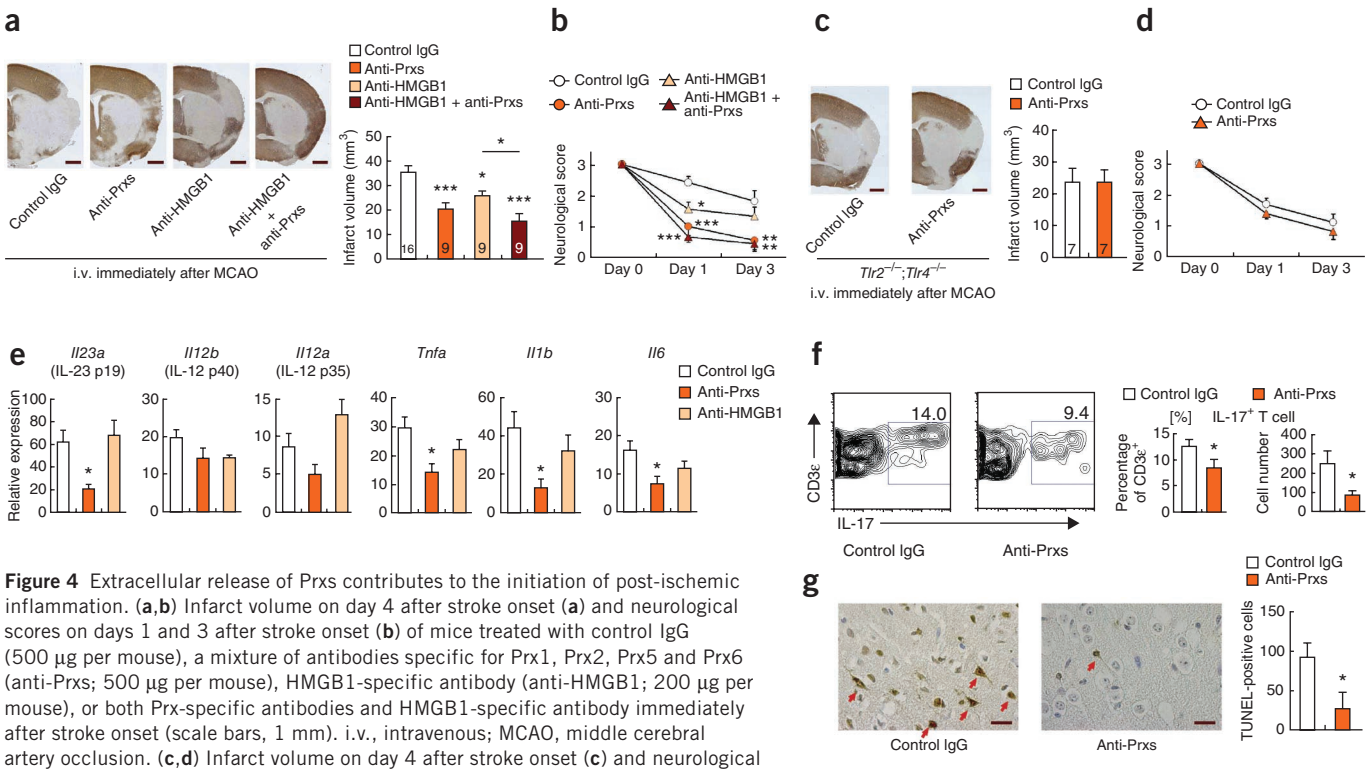

Figure 4 Extracellular release of Prxs contributes to the initiation of post-ischemic inflammation. (**a**,**b**) Infarct volume on day 4 after stroke onset (**a**) and neurological scores on days 1 and 3 after stroke onset (**b**) of mice treated with control IgG (500 μg per mouse), a mixture of antibodies specific for Prx1, Prx2, Prx5 and Prx6 (anti-Prxs; 500 μg per mouse), HMGB1-specific antibody (anti-HMGB1; 200 μg per mouse), or both Prx-specific antibodies and HMGB1-specific antibody immediately after stroke onset (scale bars, 1 mm). i.v., intravenous; MCAO, middle cerebral artery occlusion. (**c**,**d**) Infarct volume on day 4 after stroke onset (**c**) and neurological scores (**d**) on days 1 and 3 after stroke onset of TLR2 and TLR4 double-deficient mice treated with control IgG or the Prx-specific antibody mixture immediately after stroke onset ($n = 7$ for each) (scale bars, 1 mm). (**e**–**g**) mRNA levels of inflammatory cytokines in brain infiltrating immune cells on day 1 after stroke onset ($n = 11$ for control IgG, $n = 7$ for Prx-specific antibodies, and $n = 8$ for HMGB1-specific antibody) (**e**), the ratio and the absolute number of IL-17$^+$ T cells on day 3 after stroke onset ($n = 8$ for each) (**f**) and the absolute number of TUNEL$^+$ cells in the peri-infarct area on day 4 after stroke onset (scale bars, 50 μm; $n = 8$ for each) (**g**) in the mice treated with control IgG, Prx-specific antibody mixture or HMGB1-specific antibody immediately after stroke onset. Each mRNA expression level indicates relative expression compared to that in sham-operated mice. The number of mice is shown on each bar (**a**,**c**). $^*P < 0.05$, $^{**}P < 0.01$, $^{***}P < 0.001$ versus control IgG-administered mice (one-way ANOVA with Dunnett's correction (**a**,**b**,**e**) or two-sided Student's t test (**c**,**d**,**f**,**g**); the error bars represent s.e.m.).

lysate, we performed an antibody-depletion assay. We observed an apparent reduction of IL-23 p19–inducing activity in sucrose-gradient fractions 2 and 3 after depletion of Prxs (**Fig. 1h**), whereas antibody depletion of HMGB1 had little effect (**Supplementary Fig. 6**). These results suggest that Prx family proteins in the brain lysate are major inducers of IL-23 expression.

Originally, Prx family proteins were described as antioxidative enzymes within cells that are neuroprotective by scavenging reactive oxygen species (ROS)[26–28]. Prxs contain one (Prx6) or two (Prx1–Prx5) conserved cysteine residues. Two-cysteine Prxs scavenge ROS in cooperation with thioredoxin[26,29,30]. However, once released from the cells, Prxs are considered to lose their antioxidant capacity because of oxidation of the cysteine residues, and the redox cycle of Prxs should not be possible[26,31]. Consistent with this notion, the disruption of cysteine residues by point mutations or iodoacetamide treatment did not affect the IL-23–inducing activity of Prx5 (**Supplementary Fig. 7**). Thus, extracellular Prxs, being independent of antioxidant activity, could function as inducers of IL-23 expression in BMDCs.

Extracellular Prxs colocalize with infiltrating macrophages

Recent reports have demonstrated that Prxs are released into the extracellular fluid after brain tissue death in rats and in humans after acute ischemic stroke[32,33]. We hypothesized that Prxs released from necrotic brain cells into the extracellular compartment function as a danger signal. The mRNA expression levels of Prxs were very high in normal brain tissue, comparable to those of the housekeeping gene hypoxanthine phosphoribosyltransferase 1 (*Hprt1*) and were increased further as a result of ischemic brain injury (**Fig. 2a**).

Immunohistochemical staining with our Prx-specific antibodies successfully detected Prx1/2 and Prx6 expression in normal brain tissues, as previously reported[34] (**Supplementary Fig. 8a**,**b**). Cerebral ischemic stress induced much stronger Prx6 expression in the infarct region than in the normal tissues (**Fig. 2b**). This increase in Prx6 expression was barely observable until 4 h after the reperfusion, and Prx6 expression was very evident on day 1 but had diminished by day 4 (**Fig. 2b**). Specific staining of Prx6 was confirmed by staining with a control nonspecific IgG, which did not exhibit any such staining patterns (**Fig. 2b**). We observed a similar increase in Prx1/2 protein staining upon ischemic stress on day 1 in wild-type (WT) mice; however, we obtained no detectable signals in *Prx1*$^{-/-}$ mice (**Supplementary Fig. 8c**), confirming the specificity of our immunohistostaining.

In the ischemic brain, we observed strong Prx6 expression in the TUNEL$^+$ infarct region (**Fig. 2c**). By using confocal laser microscopy, we found that Prx6-positive, debris-like granules were abundant around TUNEL$^+$ cells in the infarct core (**Fig. 2d**). These observations indicate that Prx6 was induced in injured ischemic cells and then released into the extracellular compartment from dying cells. Notably, Prx6$^+$ debris was often observed to be co-localized with the

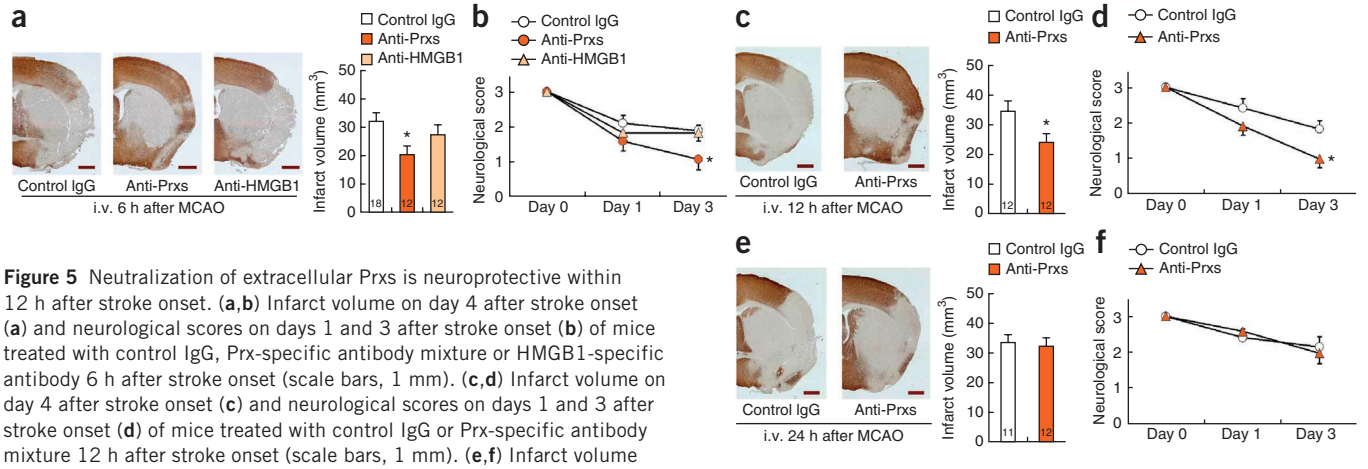

Figure 5 Neutralization of extracellular Prxs is neuroprotective within 12 h after stroke onset. (**a**,**b**) Infarct volume on day 4 after stroke onset (**a**) and neurological scores on days 1 and 3 after stroke onset (**b**) of mice treated with control IgG, Prx-specific antibody mixture or HMGB1-specific antibody 6 h after stroke onset (scale bars, 1 mm). (**c**,**d**) Infarct volume on day 4 after stroke onset (**c**) and neurological scores on days 1 and 3 after stroke onset (**d**) of mice treated with control IgG or Prx-specific antibody mixture 12 h after stroke onset (scale bars, 1 mm). (**e**,**f**) Infarct volume on day 4 after stroke onset (**e**) and neurological scores on days 1 and 3 after stroke onset (**f**) of mice treated with control IgG or Prx-specific antibody mixture 24 h after stroke onset (scale bars, 1 mm). The number of mice is shown on each bar (**a**,**c**,**e**). $^*P < 0.05$ versus control IgG–administered mice (one-way ANOVA with Dunnett's correction (**a**,**b**) or two-sided Student's *t* test (**c**–**f**); the error bars represent s.e.m.).

cell membranes of F4/80$^+$ macrophages (**Fig. 2e**,**f**), supporting our hypothesis that the extracellular release of Prx6 stimulates infiltrating macrophages.

Prxs induce IL-23 expression via TLR2 and TLR4

TLR2 and TLR4 have been implicated in ischemic brain injury[35]. Thus, we tried to determine the relationship between the IL-23–inducing activity of Prxs and TLR2 and TLR4. The recombinant Prx–mediated induction of IL-23 p19 expression was lower in TLR2- and TLR4-deficient BMDCs and completely absent in BMDCs doubly deficient in TLR2 and TLR4 as compared to WT BMDCs (**Fig. 3a**). In addition, we confirmed that Prx5 protein activated nuclear factor-κB through TLR4 in 293 cells expressing TLR4 (**Supplementary Fig. 9**). Therefore, Prxs induced IL-23 expression by activating both TLR2 and TLR4 *in vitro*.

Next, we examined inflammatory cytokine expression in the infiltrated mononuclear cells collected by Percoll-gradient centrifugation from the ischemic brain of mice deficient in TLR2, TLR4 or both. The expression levels of IL-23 p19, tumor necrosis factor-α (TNF-α) and IL-1β in the infiltrating immune cells on day 1 after stroke onset were largely dependent on both TLR2 and TLR4, but that of IL-12 p35 was not (**Fig. 3b**) (physiological data and cerebral blood flow (CBF) are shown in **Supplementary Tables 2** and **3**). Inflammatory cytokine expression was more severely reduced in TLR2 and TLR4 double-knockout mice than in TLR2 or TLR4 single-knockout mice (**Fig. 3b**), suggesting a functional redundancy between TLR2 and TLR4. In peripheral blood monocytes, we observed minimal expression of IL-23 p19, TNF-α and IL-1β (**Supplementary Fig. 10**), indicating that the activation of infiltrated cells via TLR2 and TLR4 occurred mainly in the ischemic brain rather than in the periphery.

The absolute number and the fraction of IL-17$^+$ T cells among infiltrated mononuclear cells on day 3 after stroke onset were also lower in TLR2 or TLR4 single-knockout mice and were further lowered in TLR2 and TLR4 double-knockout mice as compared to WT mice (**Fig. 3c**). However, TLR2 and TLR4 double deficiency did not significantly decrease the absolute number of interferon-γ$^+$ T cells (**Supplementary Fig. 11**); this observation is consistent with the minimal effect of TLR2 and TLR4 double deficiency on IL-12 expression. Bone marrow chimera experiments also confirmed that the infiltrating macrophages, but not residential microglia, were responsible for TLR2- and TLR4-mediated ischemic brain injury (**Fig. 3d**) and inflammatory cytokine expression (**Supplementary Fig. 12**) (CBF is shown in **Supplementary Table 4**). Thus, these data suggest that both TLR2 and TLR4 play essential parts in inducing post-ischemic inflammation by regulating the IL-23–IL-17 axis but not the IL-12–interferon-γ axis.

Extracellular Prxs trigger post-ischemic inflammation

Next, we investigated the therapeutic effects of neutralizing Prxs or HMGB1 by administrating antibodies immediately after stroke onset. The administration of a mixture of antibodies specific for Prx1, Prx2, Prx5 and Prx6, but not control IgG, had a neuroprotective effect associated with a significant reduction in infarct volume (**Fig. 4a**,**b**) (CBF and survival rate are shown in **Supplementary Table 5**). This reduction could still be observed on day 7 (**Supplementary Fig. 13**). We also confirmed that these Prx-specific antibodies were delivered to the ischemic brain tissue (**Supplementary Fig. 14**). Suppression of infarct volume growth by administering Prx-specific antibodies was dependent on TLR2, TLR4 and IL-23 (**Fig. 4c**,**d** and **Supplementary Fig. 15**). The administration of the Prx-specific antibody mixture decreased inflammatory cytokine expression in infiltrating immune cells on day 1 after stroke onset (**Fig. 4e**), as well as the absolute number and the fraction of IL-17–producing T cells on day 3 after stroke onset (**Fig. 4f** and **Supplementary Fig. 16**). The number of TUNEL$^+$ cells in the peri-infarct region on day 4 after stroke onset was also decreased by administration of the Prx-specific antibody mixture (**Fig. 4g**). These results were consistent with our hypothesis that extracellular Prxs induce the IL-23–IL-17 inflammatory pathway through TLR2 and TLR4 and promote post-ischemic inflammation and infarct volume growth.

HMGB1 is another important DAMP in ischemic brain injury[20]. We confirmed that HMGB1-specific antibody administered immediately after stroke onset reduced infarct volume (**Fig. 4a**). We obtained additive therapeutic effects by administering both Prx-specific antibodies and HMGB1-specific antibody (**Fig. 4a**,**b**). However, HMGB1-specific antibody had little effect on suppressing inflammatory cytokine expression on day 1 after stroke onset compared with the Prx-specific antibodies (**Fig. 4e**). This can be explained by the fact that extracellular release of HMGB1 is mostly diminished in the ischemic brain within 6 h after stroke onset[20], although the increase in blood cell infiltration mostly occurs 1 d after stroke onset[11].

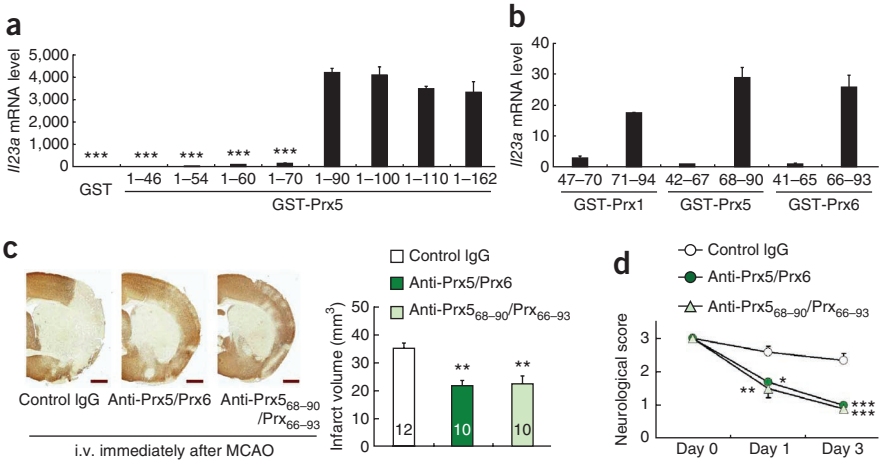

Figure 6 The conserved region of peroxiredoxins was essential for IL-23-inducing activity and the increase in infarct size. (**a**) IL-23 p19–inducing activities of C-terminal deletion mutants of Prx5 ($n = 3$ for each). The number of amino acid residues contained in each GST-fusion Prx5 peptide is shown on the *x* axis. (**b**) IL-23 p19–inducing activities of GST-fusion Prx1, Prx5, and Prx6 peptides ($n = 3$ for each). The number of amino acid residues contained in each Prx1, Prx5 and Prx6 peptide is shown on the *x* axis (GST-Prx1$_{47–70}$, GST-Prx5$_{42–67}$ and GST-Prx6$_{41–65}$ peptides contained the α2 helix region; GST-Prx1$_{71–94}$, GST-Prx5$_{68–90}$ and GST-Prx6$_{66–93}$ peptides contained the β_4 sheet and α_3 helix regions). IL-23 p19 mRNA levels were detected by means of quantitative RT-PCR in BMDCs 1 h after stimulation with 1 μM recombinant proteins and are shown relative to those of untreated BMDCs. (**c**,**d**) Infarct volume on day 4 after stroke onset (scale bars, 1 mm) (**c**) and neurological scores (**d**) on days 1 and 3 after stroke onset of mice treated with control IgG, a Prx5- and Prx6-specific antibody mixture (anti-Prx5/Prx6) or a Prx5$_{68–90}$- and Prx6$_{66–93}$-specific (common α_3 helix and β_4 sheet region) antibody mixture (anti-Prx5$_{68–90}$/Prx6$_{66–93}$) immediately after the induction of brain ischemia (300 μg per mouse). The number of mice is shown on each bar in **c**. $^*P < 0.05$, $^{**}P < 0.01$, $^{***}P < 0.001$ versus GST-Prx5$_{1–162}$ (**a**) and control IgG-treated mice (**c**,**d**) (one-way ANOVA with Dunnett's correction; the error bars represent s.e.m.).

Finally, we examined the effect of antibodies administered several hours after stroke onset to determine the therapeutic time window. Administration of the Prx-specific antibodies mixture 6 h after stroke onset significantly attenuated ischemic brain damage, whereas administration of the HMGB1-specific antibody was much less effective at this time point (**Fig. 5a**,**b**). The Prx-specific antibody mixture was therapeutic up to 12 h after stroke onset (**Fig. 5c**,**d**); however, we did not observe a therapeutic effect when it was administered 24 h after stroke onset (**Fig. 5e**,**f**). These results suggest that Prxs act later than HMGB1 in post-ischemic brain injury.

The conserved region of Prx is essential for IL-23 induction

As shown in **Figure 1f**, all Prx family proteins potently activate BMDCs. We thus suspected that a particular structure common to Prxs stimulates TLR2 and TLR4. By generating deletion mutants of Prx5, we found that the IL-23–inducing activity was located between amino acid residues 70 and 90 of Prx5 (**Fig. 6a**). This region is located at the surface of Prxs and contains β_4 sheet and α_3 helix regions that are well conserved among Prxs as well as among various species[36–38] (**Supplementary Fig. 17a**,**b**). A GST-fusion of this conserved region of Prx1, Prx5 and Prx6, but not other regions, resulted in similar IL-23–inducing activity to each other (**Fig. 6b** and **Supplementary Fig. 17c–e**).

Next, we generated specific antibodies to these conserved β_4 sheet and α_3 helix regions of Prx5 and Prx6 (Prx5$_{68–90}$ and Prx6$_{66–93}$). Although these two antibodies did not cross-react with each other (**Supplementary Fig. 18**), administration of a mixture of the Prx5$_{68–90}$-specific and Prx6$_{66–93}$-specific antibodies immediately after stroke onset significantly reduced the infarct volume on day 4 and the severity of neurological deficits on days 1 and 3 after stroke onset (**Fig. 6c**,**d**). These results suggest that this conserved region of Prxs is responsible for the induction of post-ischemic inflammation and could be an ideal target for developing neuroprotective therapy.

DISCUSSION

ROS and their inducers have been considered to be endogenous danger signals[39]. Unexpectedly, our study demonstrated that antioxidant proteins themselves can function as DAMPs under conditions of sterile inflammation. A recent study revealed that TLRs could be stimulated by DNA or formyl peptide complex released from mitochondria, which are evolutionary endosymbionts derived from bacteria[18]. Similarly, because Prxs are highly conserved among various species from bacteria to mammals, it is possible that these molecules function as DAMPs recognized by TLRs. As the conserved regions of Prxs were sufficient for induction of IL-23 expression, even partially degraded Prxs could function as DAMPs. Furthermore, the expression of Prx family proteins, in particular Prx5 and Prx6, is especially high in brain compared to other organs[30]. These are potential reasons for why Prxs could function as DAMPs in ischemic brain.

We showed that Prx-mediated post-ischemic inflammation was dependent on TLR2 and TLR4, which seem to be functionally redundant in the context of ischemic damage. Although it is rare that one TLR ligand activates multiple TLRs, HMGB1 has been shown to function as a DAMP through TLR2, TLR4 and TLR9 (refs. 15,40). The molecular mechanism underlying TLR2 and TLR4 activation by Prxs and other endogenous DAMPs remains to be clarified. It is also possible that other pattern recognition receptors (CD36, RAGE or SRA) in addition to TLRs are involved in the recognition of endogenous DAMPs and modification of TLR signaling[41–43].

Prx family proteins are antioxidant enzymes within cells, and are essential for cell survival in brain and other organ injuries[27,28,44]. Indeed, we observed the exacerbation of ischemic brain injury in *Prx1*$^{-/-}$ mice (data not shown). Yet this study revealed that once Prxs are released from necrotic brain cells into the extracellular compartment, these extracellular Prxs act as a neurotoxic danger signal via TLR2 and TLR4. Thus, we propose two opposing functions of Prx: one inside and one outside of brain cells (**Supplementary Fig. 19a**). These two opposing functions performed by a single molecule may be apposite for self-protection against injury and infection.

HMGB1 is another key DAMP that contributes to blood-brain barrier breakdown[20]. Although neutralization of HMGB1 is neuroprotective[45], extracellular HMGB1 may not be a good therapeutic target for reducing inflammation, given that the extracellular release of HMGB1 decreases rapidly in the ischemic core[20,46]. Our research demonstrates

that the extracellular release of Prxs is relatively slow and is a pivotal step in the activation of infiltrating macrophages, rather than release of HMGB1. In summary, we propose that there is a time lag as well as functional differences between HMGB1 and Prxs (**Supplementary Fig. 19b**). HMGB1 is a primary DAMP in the hyperacute phase of post-ischemic inflammation, whereas extracellular Prx is a secondary one in the acute phase of brain ischemia. The extracellular Prxs could be a more potent therapeutic target than HMGB1 because their therapeutic time window would be longer than that of HMGB1.

METHODS

Methods and any associated references are available in the online version of the paper.

Note: Supplementary information is available in the online version of the paper.

ACKNOWLEDGMENTS

We thank N. Saito, N. Shiino and M. Asakawa for technical assistance. This work was supported by special grants-in-aid (A) and open research for young academics and specialists from the Ministry of Education, Culture, Sports, Science and Technology of Japan, PRESTO and CREST from the Japan Science and Technology Agency, an Intramural Research Grant (22-4) for Neurological and Psychiatric Disorders of the National Center of Neurology and Psychiatry (NCNP), the SENSHIN Research Foundation, the Takeda Science Foundation, the Uehara Memorial Foundation, the Mochida Memorial Foundation, the Scientific Research Fund from the Ministry of Health, Labor and Welfare of Japan (09156274) and the Program for Promotion of Fundamental Studies in Health Science of the National Institute of Biomedical Innovation.

AUTHOR CONTRIBUTIONS

T. Shichita designed and performed experiments, analyzed data and wrote the manuscript; E.H. and A.K. performed TLR-deficient mouse analysis; R.M., R.S. and T. Sekiya participated in data analysis and discussion; I.T. provided specific input on protein analysis; H.O. and T.K. provided technical advice about experimental design; T.Y. and T.I. provided crucial input on Prx1's functions; H.T., S.M. and M.N. provided the HMGB1-specific antibody and crucial input on HMGB1; K.K. provided specific input regarding LC-MS analysis; K.M. and S.A. provided TLR2 and/or TLR4-deficient mice; A.Y. initiated and directed the entire study, designed experiments and wrote the manuscript.

COMPETING FINANCIAL INTERESTS

The authors declare no competing financial interests.

Published online at http://www.nature.com/doifinder/10.1038/nm.2749.
Reprints and permissions information is available online at http://www.nature.com/reprints/index.html.

1. Moskowitz, M.A., Lo, E.H. & Iadecola, C. The science of stroke: mechanisms in search of treatments. *Neuron* **67**, 181–198 (2010).
2. Lo, E.H. Degeneration and repair in central nervous system disease. *Nat. Med.* **16**, 1205–1209 (2010).
3. Ooboshi, H. *et al.* Postischemic gene transfer of interleukin-10 protects against both focal and global brain ischemia. *Circulation* **111**, 913–919 (2005).
4. Macrez, R. *et al.* Stroke and the immune system: from pathophysiology to new therapeutic strategies. *Lancet Neurol.* **10**, 471–480 (2011).
5. Iadecola, C. & Anrather, J. The immunology of stroke: from mechanisms to translation. *Nat. Med.* **17**, 796–808 (2011).
6. Eltzschig, H.K. & Eckle, T. Ischemia and reperfusion—from mechanism to translation. *Nat. Med.* **17**, 1391–1401 (2011).
7. Hurn, P.D. *et al.* T- and B-cell–deficient mice with experimental stroke have reduced lesion size and inflammation. *J. Cereb. Blood Flow Metab.* **27**, 1798–1805 (2007).
8. Liesz, A. *et al.* Inhibition of lymphocyte trafficking shields the brain against deleterious neuroinflammation after stroke. *Brain* **134**, 704–720 (2011).
9. Yilmaz, G., Arumugam, T.V., Stokes, K.Y. & Granger, D.N. Role of T lymphocytes and interferon-gamma in ischemic stroke. *Circulation* **113**, 2105–2112 (2006).
10. Ren, X. *et al.* Regulatory B cells limit CNS inflammation and neurologic deficits in murine experimental stroke. *J. Neurosci.* **31**, 8556–8563 (2011).
11. Shichita, T. *et al.* Pivotal role of cerebral interleukin-17-producing γδT cells in the delayed phase of ischemic brain injury. *Nat. Med.* **15**, 946–950 (2009).
12. Konoeda, F. *et al.* Therapeutic effect of IL-12/23 and their signaling pathway blockade on brain ischemia model. *Biochem. Biophys. Res. Commun.* **402**, 500–506 (2010).
13. Tang, S.C. *et al.* Pivotal role for neuronal Toll-like receptors in ischemic brain injury and functional deficits. *Proc. Natl. Acad. Sci. USA* **104**, 13798–13803 (2007).
14. Chen, C.J. *et al.* Identification of a key pathway required for the sterile inflammatory response triggered by dying cells. *Nat. Med.* **13**, 851–856 (2007).
15. Yanai, H. *et al.* HMGB proteins function as universal sentinels for nucleic-acid-mediated innate immune responses. *Nature* **462**, 99–103 (2009).
16. Marsh, B.J., Williams-Karnesky, R.L. & Stenzel-Poore, M.P. Toll-like receptor signaling in endogenous neuroprotection and stroke. *Neuroscience* **158**, 1007–1020 (2009).
17. Stewart, C.R. *et al.* CD36 ligands promote sterile inflammation through assembly of a Toll-like receptor 4 and 6 heterodimer. *Nat. Immunol.* **11**, 155–161 (2010).
18. Zhang, Q. *et al.* Circulating mitochondrial DAMPs cause inflammatory responses to injury. *Nature* **464**, 104–107 (2010).
19. Rivest, S. Regulation of innate immune responses in the brain. *Nat. Rev. Immunol.* **9**, 429–439 (2009).
20. Zhang, J. *et al.* Anti–high mobility group box-1 monoclonal antibody protects the blood-brain barrier from ischemia-induced disruption in rats. *Stroke* **42**, 1420–1428 (2011).
21. Kim, J.B. *et al.* HMGB1, a novel cytokine-like mediator linking acute neuronal death and delayed neuroinflammation in the postischemic brain. *J. Neurosci.* **26**, 6413–6421 (2006).
22. Yang, Q.W. *et al.* HMBG1 mediates ischemia-reperfusion injury by TRIF-adaptor independent Toll-like receptor 4 signaling. *J. Cereb. Blood Flow Metab.* **31**, 593–605 (2011).
23. Hayakawa, K., Qiu, J. & Lo, E.H. Biphasic actions of HMGB1 signaling in inflammation and recovery after stroke. *Ann. NY Acad. Sci.* **1207**, 50–57 (2010).
24. Riddell, J.R., Wang, X.Y., Minderman, H. & Gollnick, S.O. Peroxiredoxin 1 stimulates secretion of proinflammatory cytokines by binding to TLR4. *J. Immunol.* **184**, 1022–1030 (2010).
25. Chesterman, E.S. *et al.* Investigation of Prx1 protein expression provides evidence for conservation of cardiac-specific posttranscriptional regulation in vertebrates. *Dev. Dyn.* **222**, 459–470 (2001).
26. Patenaude, A., Murthy, M.R. & Mirault, M.E. Emerging roles of thioredoxin cycle enzymes in the central nervous system. *Cell. Mol. Life Sci.* **62**, 1063–1080 (2005).
27. Hu, X. *et al.* Peroxiredoxin-2 protects against 6-hydroxydopamine–induced dopaminergic neurodegeneration via attenuation of the apoptosis signal-regulating kinase (ASK1) signaling cascade. *J. Neurosci.* **31**, 247–261 (2011).
28. Rashidian, J. *et al.* Essential role of cytoplasmic cdk5 and Prx2 in multiple ischemic injury models, *in vivo*. *J. Neurosci.* **29**, 12497–12505 (2009).
29. Wood, Z.A., Schröder, E., Robin Harris, J. & Poole, L.B. Structure, mechanism and regulation of peroxiredoxins. *Trends Biochem. Sci.* **28**, 32–40 (2003).
30. Seo, M.S. *et al.* Identification of a new type of mammalian peroxiredoxin that forms an intramolecular disulfide as a reaction intermediate. *J. Biol. Chem.* **275**, 20346–20354 (2000).
31. Toohey, J.I. Sulfhydryl dependence in primary explant hematopoietic cells. Inhibition of growth *in vitro* with vitamin B12 compounds. *Proc. Natl. Acad. Sci. USA* **72**, 73–77 (1975).
32. Chou, J.L. *et al.* Proteomic investigation of a neural substrate intimately related to brain death. *Proteomics* **11**, 239–248 (2011).
33. Dayon, L. *et al.* Brain extracellular fluid protein changes in acute stroke patients. *J. Proteome Res.* **10**, 1043–1051 (2011).
34. Jin, M.H. *et al.* Characterization of neural cell types expressing peroxiredoxins in mouse brain. *Neurosci. Lett.* **381**, 252–257 (2005).
35. Brea, D. *et al.* Toll-like receptors 2 and 4 in ischemic stroke: outcome and therapeutic values. *J. Cereb. Blood Flow Metab.* **31**, 1424–1431 (2011).
36. Hirotsu, S. *et al.* Crystal structure of a multifunctional 2-Cys peroxiredoxin heme-binding protein 23kDa/proliferation-associated gene product. *Proc. Natl. Acad. Sci. USA* **96**, 12333–12338 (1999).
37. Declercq, J.P. *et al.* Crystal structure of human peroxiredoxin 5, a novel type of mammalian peroxiredoxin at 1.5 A resolution. *J. Mol. Biol.* **311**, 751–759 (2001).
38. Choi, H.J. *et al.* Crystal structure of a novel human peroxidase enzyme at 2.0 A resolution. *Nat. Struct. Biol.* **5**, 400–406 (1998).
39. Chen, G.Y. & Nuñez, G. Sterile inflammation: sensing and reacting to damage. *Nat. Rev. Immunol.* **10**, 826–837 (2010).
40. Yu, M. *et al.* HMGB1 signals through Toll-like receptor (TLR) 4 and TLR2. *Shock* **26**, 174–179 (2006).
41. Triantafilou, M. *et al.* Membrane sorting of Toll-like receptor (TLR)-2/6 and TLR2/1 heterodimers at the cell surface determines heterotypic associations with CD36 and intracellular targeting. *J. Biol. Chem.* **281**, 31002–31011 (2006).
42. Yi, H. *et al.* Pattern recognition scavenger receptor SRA/CD204 down-regulates Toll-like receptor 4 signaling–dependent CD8 T-cell activation. *Blood* **113**, 5819–5828 (2009).
43. Akashi-Takamura, S. & Miyake, K. TLR accessory molecules. *Curr. Opin. Immunol.* **20**, 420–425 (2008).
44. Eismann, T. *et al.* Peroxiredoxin-6 protects against mitochondrial dysfunction and liver injury during ischemia-reperfusion in mice. *Am. J. Physiol. Gastrointest. Liver Physiol.* **296**, G266–G274 (2009).
45. Liu, K. *et al.* Anti-high mobility group box 1 monoclonal antibody ameliorates brain infarction induced by transient ischemia in rats. *FASEB J.* **21**, 3904–3916 (2007).
46. Qiu, J. *et al.* Early release of HMGB-1 from neurons after the onset of brain ischemia. *J. Cereb. Blood Flow Metab.* **28**, 927–938 (2008).

ONLINE METHODS

Mice. TLR2 knockout, TLR4 knockout, TLR2 and TLR4 double-knockout, and MyD88-knockout mice were provided by K.M. and S.A. Prx1-knockout mice were provided by T.I. All mice were on a C57BL/6 background. All experiments were approved by the Institutional Animal Research Committee of Keio University (approval number: 08004).

Mouse focal brain ischemia model. Male mice, aged 9–12 weeks and weighing 20–30 g, were used for focal brain ischemia experiments. There was no significant difference in weight and age between WT mice and any of the knockout groups. We used a transient middle cerebral artery occlusion (MCAO) model induced by means of an intraluminal suture. The method of inducing this transient suture MCAO model has been described previously[11,47]. A >60% reduction in cerebral blood flow was confirmed by laser Doppler flowmetry, and head temperature was kept at 36 °C using a heat lamp. Sixty minutes after MCAO, the brain was reperfused by the withdrawal of the intraluminal suture.

Preparation and LC-MS analysis of brain lysate. The mice were perfused with PBS transcardially. The forebrain was removed, homogenized with RPMI-1640 and centrifuged at 15,000 r.p.m. for 5 min. The supernatant was made up to 1 ml with RPMI-1640 and used as the brain lysate. For the pronase and DNase I digestion assay, the brain lysate was incubated with pronase (1–10 U ml^{-1}, Roche) or DNase I (50 μg ml^{-1}, Roche) at 37 °C for 1 h.

For the sucrose density gradient centrifugation and LC-MS analysis, the brain lysate was ultracentrifuged at 47,000 r.p.m. for 1 h. The supernatant was applied to DEAE Sepharose Fast Flow columns (GE Healthcare), and the flow-through was condensed by ultrafiltration with an Amicon Ultra-4 Centrifugal Filter Unit with Ultracel-10 membrane (Millipore). Four hundred microliters of condensed solution was layered on a 1-ml 10–40% (w/w) linear sucrose gradient in PBS and centrifuged at 40,000 r.p.m. for 12 h. Sucrose was depleted by ultrafiltration from each of the sucrose gradient fractions. We added each of the sucrose-gradient fractions to a culture of BMDCs to examine its capacity to induce inflammatory cytokine expression and analyzed sucrose gradient fractions 1–4 by means of LC-MS. LC-MS analysis was performed after trypsin treatment using a Qstar-XL mass spectrometer (Applied Biosystems).

For the antibody-depletion assay, HMGB1 or Prx proteins were depleted by immunoprecipitation with antibody–cross-linked Protein G beads using dimethyl pimelimidate. Depletion of HMGB1 or Prx proteins from the brain lysate was confirmed by western blot analysis.

Generation of recombinant protein. cDNA clones encoding candidate proteins identified by LC-MS analysis were cloned from a mouse brain cDNA library. All mutations were made with complementary mutagenic oligonucleotides. Final cDNA constructs were inserted into the pGEX6P-3 plasmid (GE Healthcare) and expressed as GST fusion proteins in BL21 competent cells (Stratagene). Following fusion protein purification using glutathione-Sepharose 4B columns (GE Healthcare), 100 μl of protein-bound glutathione beads were extensively washed with 10 ml of cold PBS five times. Washed protein-bound glutathione beads were either eluted with 20 mM reduced glutathione (pH 8.0) to elute GST-fusion proteins or incubated with PreScission Protease (GE Healthcare) overnight at 4 °C to remove the GST tag. Finally, these recombinant proteins were incubated with Affi-Prep Polymyxin Support (Bio-Rad) for 12 h at 4 °C to remove endotoxins and endotoxin-bound proteins. We confirmed through SDS-PAGE and Coomassie brilliant blue staining that the same amounts of purified recombinant proteins were applied to BMDC stimulation experiments. Recombinant GST protein was always used as a negative control for cytokine induction in BMDCs.

To generate alkylated Prx proteins, recombinant Prx protein with 1 mM dithiothreitol was incubated with 55 mM iodoacetamide (Wako Pure Chemical Industries) in a dark chamber at room temperature for 1 h. Sufficient alkylation of –SH on cysteine residues in Prx protein was confirmed using dithionitrobenzoic acid (Dojindo Laboratories).

Generation of rabbit polyclonal antibody. Rabbits were immunized with recombinant Prx proteins by Japan Lamb. To affinity-purify antibodies, recombinant Prx proteins were crosslinked to *N*-hydroxysuccinimide (NHS)-Sepharose beads. The protein A–purified antibodies from immunized rabbit serum were applied to Prx protein-bound NHS-Sepharose beads. These affinity-purified antibodies were used for all experiments in this study.

HMGB1-specific antibody. HMGB1-specific antibody (rat, monoclonal) was kindly provided by H.T., S.M. and M.N. As previously reported, 200 μg of HMGB1-specific antibody was administered immediately or 6 h after the induction of brain ischemia[20,45].

Statistical analyses. Data are expressed as means ± s.e.m. We performed a one-way ANOVA followed by *post hoc* multiple-comparison tests (Dunnett's correction) to analyze differences among three or more groups of mice. Between two groups of mice, an unpaired Student's *t* test was performed to determine statistical significance. $P < 0.05$ was considered a significant difference.

Additional methods. Detailed methodology is described in the **Supplementary Methods**.

47. Sugimori, H. *et al.* Krypton laser-induced photothrombotic distal middle cerebral artery occlusion without craniectomy in mice. *Brain Res Brain Res. Protoc.* **13**, 189–196 (2004).

doi:10.1038/nm.2749